Biochemical and Biophysical Research Communications 450 (2014) 464–469

Contents lists available at ScienceDirect

Biochemical and Biophysical Research Communications

journal homepage: www.elsevier.com/locate/ybbrc

Molecular mechanism regulating myosin and cardiac functions by ELC

Janine Lossie [a,1], Clemens Köhncke [a,1], Shokoufeh Mahmoodzadeh [b,c,1], Walter Steffen [d], Monica Canepari [e], Manuela Maffei [e], Martin Taube [c], Oriane Larchevêque [c], Philipp Baumert [f], Hannelore Haase [c], Roberto Bottinelli [e,g], Vera Regitz-Zagrosek [b], Ingo Morano [c,h,*]

[a] University Medicine Berlin Charité, Experimental and Clinical Research Center (ECRC), Germany
[b] University Medicine Berlin Charité, Institute of Gender in Medicine, Germany
[c] Max-Delbrueck-Center for Molecular Medicine, Berlin, Germany
[d] Medizinische Hochschule Hannover, Institut fuer Molekular- und Zellphysiologie, Germany
[e] Department of Molecular Medicine and Sport Medicine Research Center, University of Pavia, Italy
[f] Johann Wolfgang Goethe-Universitaet, Institut für Sportwissenschaften, Frankfurt/Main, Germany
[g] Fondazione Salvatore Maugeri, Scientific Institute of Pavia, Pavia, Italy
[h] University Medicine Berlin Charité, Germany

ARTICLE INFO

Article history:
Received 16 May 2014
Available online 6 June 2014

Keywords:
Essential myosin light chains
Myosin
Stiffness
In vitro motility
Mutations

ABSTRACT

The essential myosin light chain (ELC) is involved in modulation of force generation of myosin motors and cardiac contraction, while its mechanism of action remains elusive. We hypothesized that ELC could modulate myosin stiffness which subsequently determines its force production and cardiac contraction. Therefore, we generated heterologous transgenic mouse (TgM) strains with cardiomyocyte-specific expression of ELC with human ventricular ELC (hVLC-1; $TgM^{hVLC\text{-}1}$) or E56G-mutated hVLC-1 (hVLC-1^{E56G}; TgM^{E56G}). hVLC-1 or hVLC-1^{E56G} expression in TgM was around 39% and 41%, respectively of total VLC-1. Laser trap and *in vitro* motility assays showed that stiffness and actin sliding velocity of myosin with hVLC-1 prepared from $TgM^{hVLC\text{-}1}$ (1.67 pN/nm and 2.3 μm/s, respectively) were significantly higher than myosin with hVLC-1^{E56G} prepared from TgM^{E56G} (1.25 pN/nm and 1.7 μm/s, respectively) or myosin with mouse VLC-1 (mVLC-1) prepared from C57/BL6 (1.41 pN/nm and 1.5 μm/s, respectively). Maximal left ventricular pressure development of isolated perfused hearts *in vitro* prepared from $TgM^{hVLC\text{-}1}$ (80.0 mmHg) were significantly higher than hearts from TgM^{E56G} (66.2 mmHg) or C57/BL6 (59.3 ± 3.9 mmHg). These findings show that ELCs decreased myosin stiffness, *in vitro* motility, and thereby cardiac functions in the order hVLC-1 > hVLC-1^{E56G} ≈ mVLC-1. They also suggest a molecular pathomechanism of hypertrophic cardiomyopathy caused by hVLC-1 mutations.

1. Introduction

Two myosin heavy chains (MyHC; 200 kDa each) and four non-covalently linked myosin light chains, two essential myosin light chains and two regulatory light chains (ELC and RLC, resp.: 16–28 kDa), form the native Type II myosin molecule, which drives muscle contraction.

The primary structure of cardiac ELC isoforms presents with an elongated N-terminal (aa 1–46), and a dumbbell-like C-terminal domain (aa 47-≈200) consisting of four helix-loop-helix EF-hand motifs [1,2]. ELCs bind with the utmost lysine-rich N-terminus to actin and with their C-terminal domain to the myosin lever arm (myosin-LA), RLC, and myosin motor domain (myosin-MD) [2,3] and emerged as an important regulatory molecule which determines chemo-mechanical transduction in muscle fibers [3–5]. Thus, myosin denuded of ELCs revealed only 1/3 of its normal force generation [5] and reduced *in vitro* actin filament sliding velocity [5,6]. Mutations of MYL3 (accession NM_000258.2), the gene encoding the human VLC-1 (hVLC-1) causing familial hypertrophic cardiomyopathy (FHC) disturbed a variety of myosin- and cardiac functions in experimental models (for review see [7]), further substantiating the important role of ELC during chemo-mechanical transduction. ELC/myosin binding suggests a structural stabilization of the compliant α-helix of the myosin-LA. This is an important functional aspect since the lever arm is considered to be the elastic element which amplifies the very small conformational changes in the motor domain to a large movement

* Corresponding author at: Max-Delbrück-Center for Molecular Medicine, Robert-Roessle-Str. 10, 13125 Berlin, Germany. Fax: +49 30 9406 2277.
E-mail address: imorano@mdc-berlin.de (I. Morano).
[1] The first three authors contributed equally to this work.

http://dx.doi.org/10.1016/j.bbrc.2014.05.142
0006-291X/

of around 5–10 nm [8]. Association of myosin with ELCs may increase the myosin-LA rigidity and at the same time would power-up force generation per cross-bridge [5,9]. In this study we tested the hypothesis that the association of myosin with different ELC (iso)forms could modulate myosin stiffness and force generation, *in vitro* motility of actin filament sliding, and thus cardiac muscle functions.

To obtain functionally intact myosin and cardiac preparations with weak myosin-binding hVLC-1^{E56G}, we generated heterologous transgenic mouse strains which overexpressed hVLC-1^{E56G} in the ventricle (TgM^{E56G}). We show that different ELC isoforms modulate myosin stiffness and force generation and subsequently cardiac contraction. These results could also provide a reasonable pathomechanism explaining the development of FHC by hVLC-1 mutations.

2. Materials and methods

2.1. Generation of transgenic mice and genotyping

All animal experiments were approved by and conducted in accordance with the guidelines set out by the State Agency for Health and Social Affairs (LaGeSo, Berlin, Germany, G 0178/07).

We generated two transgenic mouse (TgM) models with cardiomyocyte-specific overexpression of the non-mutated human ventricular ELC (hVLC-1) or its E56G mutated form (hVLC-1^{E56G}), i.e. TgM^{hVLC-1} and TgM^{E56G}, respectively (for more details see the Supplemental data).

Cardiac morphology was assessed by echocardiography (Vevo2100, VisualSonics, Toronto, Canada) of 3 month old male TgM^{hVLC-1}, TgM^{E56G} and C57BL/6 mice under light isoflurane (2%) anaesthesia.

For tissue isolation, 3 months old male transgenic mice were anaesthetized using ketamine hydrochloride (80 mg/ml)/xylazine hydrochloride (12 mg/ml) administered by i.p.-injection (1 mg/kg body weight).

2.2. Transcriptome analysis

Total RNA was extracted from ventricles of 3 month old male TgM^{hVLC-1} or TgM^{E56G} ($n = 4$ animals/group) using TRIzol reagent, and transcribed into cDNA with Two-Cycles Target labeling and Control Reagents (Ambion WT Expression Kit and GeneChip WT Terminal Labeling and Hybridization kit, Affymetrix, Santa Clara, CA, USA). Non-pooled microarray experiments were performed with cDNA using GeneChip Mouse Gene 1.0 ST Array (28,853 genes, Affymetrix). For comparison of the expression profiles of TgM^{hVLC-1} with TgM^{E56G}, we considered a False Discovery Rate (FDR-value) of <0.05 and a changed expression level >2.0-fold as significant (for more details see Supplemental data).

2.3. Transgene incorporation into myosin

We prepared myofibrils according to [10] and ventricular myosin according to [11]. Transgene expression of myosin preparation was evaluated by densitometrical scanning of the Coomassie-stained protein bands and expressed as % of hVLC-1 or hVLC-1^{E56G} of total VLC-1 (transgenic hVLC-1 + endogenous mVLC-1 = 100%) using ImageJ.

2.4. Analysis of myosin heavy chain isoenzyme expression

Myosin heavy chain (MyHC) isoenzyme expression pattern was analyzed from ventricular myofibrils by a modified method according to [12]. Briefly, myofibrils were dissolved in 2% SDS and loaded (3 μg/lane) on a SDS–PAGE consisting of a 6% separation gel containing 10% glycerol for 15 h at 50 V const. in the cold room. Gels were stained with Coomassie-blue.

2.5. Laser-trap analysis

Measurements of the motor mechanics including motor stiffness of single myosins were carried out using an optical trap approach. The optical trapping set-up was based on a Zeiss Axiovert microscope described elsewhere [13]. The positions of the two traps were controlled by electro-optical deflectors (EOD), which were used to move the 2 bead-actin filament-dumbbell relative to the myosin molecule. Actomyosin binding events were detected using the variance-Hidden Markov procedure [14], which gave estimates of the stiffness of each actin-bead linkage and the myosin head. The stiffness of the links was very non-linear and a minimum tension, typically 10 pN, was required for significant noise reduction during myosin binding. To achieve relatively high link stiffness between latex beads and actin filament, we stretched the dumbbell by moving the trapped beads apart at a laser power giving a trap stiffness of about 0.1 pN/nm. The total stiffness along the *x*-axis of the free dumbbell was then reduced by using a positive feedback system in AC mode as previously described [15] (for more details see Supplemental data).

2.6. In vitro motility assay

Myosin was extracted from glycerinated left ventricular myocardium of TgM^{hVLC-1}, TgM^{E56G}, and C57BL/6 mice and analyzed in the *in vitro* motility assay (IVMA) as described previously [16]. To remove the rigor-like heads from the myosin preparation, after washing out the unbound myosin with bovine serum albumin, the flow cell was washed with two volumes of a solution of 5 μM phalloidin-labeled actin, allowed to incubate for 1–2 min, then washed with 2 volumes of buffer containing 1 mM ATP followed by a wash with experimental buffer (25 mM MOPS, 25 mM KCl, 4 mM $MgCl_2$, 1 mM EGTA, 1 mM DTT, 200 μg/ml glucose oxidase, 36 μg/ml catalase, 5 mg/ml glucose, and 2 mM ATP (pH 7.2 at 25 °C)). Actin sliding velocities (Vf) were measured and their distribution characterized according to parametric statistics [16].

2.7. Skinned fiber analysis

Demembranated multicellular heart fibers (skinned fibers) were prepared from ventricles of TgM^{hVLC-1} or TgM^{E56G} as described [17]. For mechanical experiments, fibers were dissected into bundles of 150–200 μm diameter and 1–1.5 mm length under a preparation microscope. Fibers were mounted isometrically between a force transducer and a length step generator (Scientific Instruments, Heidelberg) with micro syringes in relaxation solution (25 mM imidazole, 10 mM ATP, 10 mM creatinphosphate, 12.5 mM $MgCl_2$, 5 mM NaN_3, 1 mM DTE, 5 mM EGTA, 12.5 mM KCl, 380U/ml creatine kinase, pH 7). Sarcomere length was at resting tension (1.95–2.0 μm) as detected by laser diffraction analysis. Contraction solution was the same as relaxation solution except that EGTA was substituted by 5 mM CaEGTA.

2.8. Isolated perfused hearts (Langendorff mode)

Hearts of narcotized animals were rapidly excised and transferred to a dissection dish containing ice-cold modified Krebs–Henseleit buffer containing 118 mM NaCl (118.0), 4.7 mM KCl, 2 mM $CaCl_2$, 2.1 mM $MgSO_4$, 24.7 mM $NaHCO_3$, 1.2 mM KH_2PO_4, 0.06 mM EDTA, and 11 mM glucose. A 21 gauge stainless steel cannula was inserted into the aorta in the cold buffer dish. Afterwards the hearts were mounted on the Langendorff perfusion rig and retrogradely perfused under constant pressure of 60 mmHg

at 37 °C. Carbogen (5% CO_2, 95% O_2) was delivered to the Krebs–Henseleit buffer to maintain a pH of 7.4. Hearts were electrically stimulated with a coaxial electrode at 414 bpm. To measure left ventricular isovolumetric pressure (LVP) a self-made fluid filled (water) balloon was inserted in the left ventricle. The balloon was connected via a fluid filled tube to a calibrated pressure transducer (APT300, Hugo Sachs Electronics (HSE) Germany). Other parameters were calculated based on the LVP such as maximum rate of pressure increase and pressure decrease (+dLVP/dtmax, −dLVP/dtmax). All data were acquired using the Isoheart software (HSE).

2.9. Statistics

Values are means ± SEM. Statistical difference between mean values was calculated using Student's *t*-test for two-tailed unpaired values or 1-way ANOVA and data were considered significant at *p*-values of <0.05.

3. Results and discussion

Five TgM^{E56G} founders and four TgM^{hVLC-1} founders were genotyped positively, i.e. revealed the expected PCR-signal of 989 bp while C57BL/6 mice showed no PCR-signal (Fig. 1A). Protein analysis of ventricular myosin obtained from TgM^{hVLC-1}, TgM^{E56G} and C57BL/6 mice by SDS–PAGE showed that the transgenic hVLC-1 forms (25 kDa) were present only in both TgM strains but not in C57BL/6 (Fig. 1B). Expression of transgenic hVLC-1 in TgM^{hVLC-1} ($n = 24$) and TgM^{E56G} mice ($n = 35$) were not significantly different (39.1 ± 1.7% and 40.7 ± 1.9%, respectively). We could only detect α-MyHC expression on the myofibrillar protein level in all mouse models investigated (Fig. 1C).

Analysis of *in vivo* cardiac morphology and contractile parameters by echocardiography revealed that three month old male TgM^{E56G} developed no cardiac hypertrophy (Supplement data, Table 1). Relative wall thickness and left ventricular mass/body weight ratio remained unchanged in both TgM strains if compared with C57BL/6 (Supplement data, Table 1). In line with our data, a hypertrophic cardiac phenotype could neither be observed in a homologous rabbit model which overexpressed M149V mutated rabbit VLC-1 [18] nor in the homologous TgM model which overexpressed M149V mutated mouse VLC-1 [19]. Likewise, a heterologous TgM model overexpressing A57G mutated hVLC-1 (TgM^{A57G}) did not develop the hypertrophic phenotype [20]. In line, stroke volume, ejection fraction, and fractional shortening were similar in TgM^{E56G}, TgM^{hVLC-1}, and C57BL/6 (Supplement data, Table 1).

We compared the gene expression profiles of the hearts prepared from 3 months old male TgM^{hVLC-1} or TgM^{E56G} by Affymetrix array experiments ($n = 4$ per group). A total amount of 32 differentially expressed genes (FDR < 0.05, expression levels >2-fold) were observed between both TgM groups (Supplemental data, Table 2). Expression of hypertrophic marker genes remained similar.

Ventricular single myosin functions TgM^{hVLC-1}, TgM^{E56G}, and C57BL/6, mice were investigated using the laser trap technology. Binding of a single myosin motor to the actin filament resulted in a pronounced reduction of the Brownian movement (reduction of the variance signal) of the dumbbell (Fig. 2A and B). Compared to myosin prepared from C57BL/6 ($n = 16$ motor molecules, 3905 events) the myosin from TgM^{hVLC-1} ($n = 30$ motor molecules, 6789 events) showed a significantly increased motor stiffness, namely from 1.41 ± 0.09 pN/nm to 1.67 ± 0.16 pN/nm. These stiffness values are in general agreement with values obtained from fiber experiments (rabbit psoas) which revealed myosin stiffness of 1.7 pN/nm [21] as well as from optical trap experiments with single myosin molecules (rabbit psoas) demonstrating a stiffness value of 1.79 pN/nm [13]. In contrast, 1.4 pN/nm and 0.4 pN/nm for fast and slow rat skeletal muscle, respectively [22], and 0.7 pN/nm for rabbit skeletal muscle myosin [23] were also

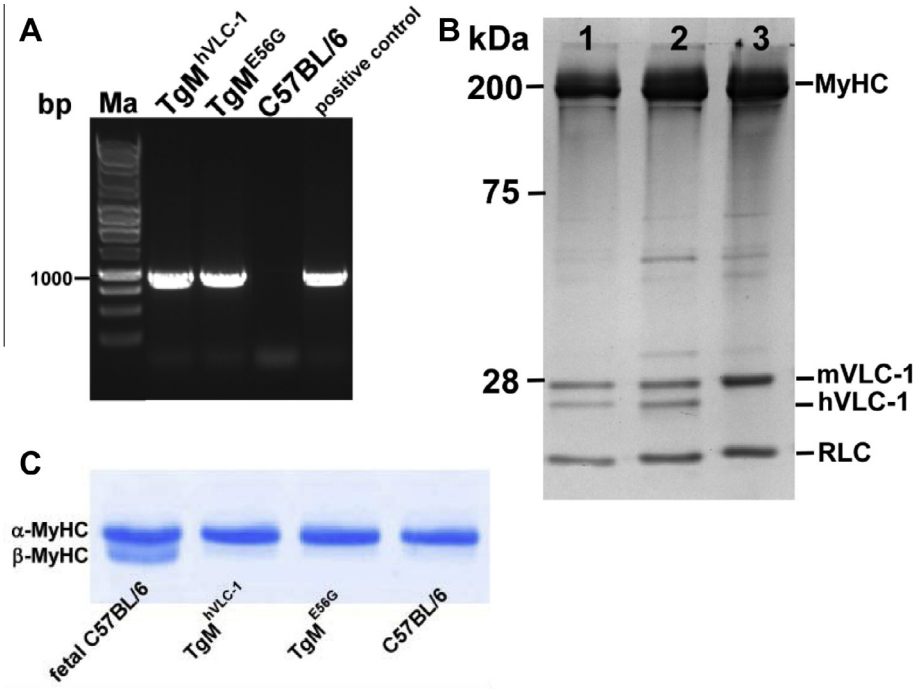

Fig. 1. Generation and characterization of transgenic mouse lines. Genomic DNA (ear biopsies) of TgMhVLC-1, TgME56G were used for transgene-specific PCR yielding a fragment of 989 bp. Construct containing hVLC-1 gene and genomic DNA obtained from C57BL/6 were used as positive and negative controls. (B) SDS–PAGE (12%) of purified ventricular myosin (1–2 μg/lane) of TgM^{hVLC-1} (Lane 1), TgM^{E56G} (Lane 2), and C57BL/6 mice (Lane 3); RLC: regulatory myosin light chain. (C) Analysis of MyHC isoenzyme expression in the myofibrils of left ventricles of male TgM^{hVLC-1}, TgM^{E56G}, and C57BL/6. A fetal mouse ventricle with both α- and β-used to identify MyHC isoenzymes.

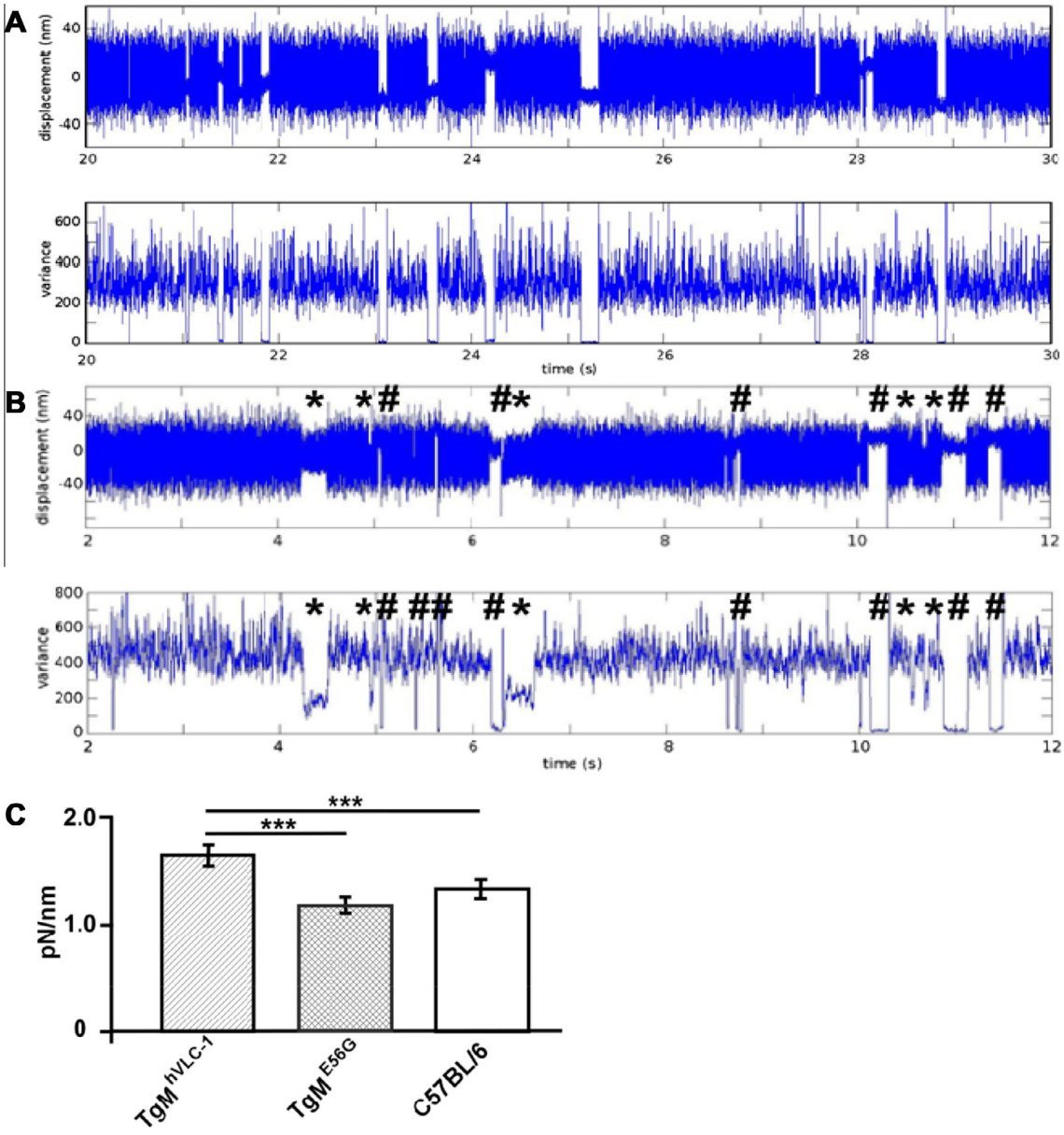

Fig. 2. Laser trap analysis. (A) Representative displacement (top) and variance (bottom) records of binding events to actin-dumbbell of ventricular myosin of TgM^{hVLC-1}. Only binding events with high motor stiffness could be observed (cf. Fig. 2C). (B) Representative displacement (top) and variance (bottom) records of two types of binding events to actin-dumbbell observed with ventricular myosin of TgM^{E56G}. Please note, that myosin motors with both high (hash mark) and low (asterisks) stiffness events in the same recording were rare observations (3 motors out of a total of 82 motors). (C) Motor stiffness of myosin purified from ventricles of 3 months old male C57BL/6, TgM^{hVLC-1}, or TgM^{E56G} using the variance/co-variance model.26 values are means ± SEM. Data were corrected to compensate for lower frequency (10 kHz) recordings40, $^{***}p < 0.001$.

reported. The mean stiffness value of myosin from TgM^{hVLC-1} seems to be underestimated, since it may represent mixed data derived from myosin with mVLC-1 and myosin with hVLC-1 (ca. 40%). Hence, myosin with hVLC-1 ought to have a higher stiffness than myosin with mVLC-1, i.e. ≈2.96 pN/nm in order to be able to increase the observed mean value from 1.41 pN/nm to 1.67 pN/nm. Compared to TgM^{hVLC-1}, ventricular myosin prepared from TgM^{E56G} revealed a significantly ($p < 0.001$) reduced mean motor stiffness of 1.25 ± 0.09 pN/nm ($n = 82$ motor molecules, 12847 events) (Fig. 2C). On closer examination of myosin with hVLC-1^{E56G}, we noticed two subgroups of motors, one with 0.28 ± 0.04 pN/nm ($n = 19$, 2857 events), significantly lower ($p < 0.001$) than myosin from C57BL/6 or TgM^{hVLC-1}, and a second group with 1.60 ± 0.08 pN/nm ($n = 63$, 9990 events), significantly ($p < 0.001$) higher compared to myosin from C57BL/6, but not to myosin from TgM^{hVLC-1} (Fig. 2B). Binding events with high stiffness produced an apparent working stroke of ~5.1 nm ($n = 242$) and the binding events with low stiffness produced an apparent working stroke of 2.5 nm ($n = 622$). Since $F = \kappa x$, with x (the working stroke) being 5.1 nm for high-stiffness motors, force generation of single myosin molecules with hVLC-1 and mVLC-1 may be around 16 pN and 7.2 pN, respectively. The species-specific gain-of-function of hVLC-1-myosin compared to mVLC-1-myosin may be based on the different primary sequences of mVLC-1 and hVLC-1 which exert different myosin-LA interaction properties. Taking a working stroke of 2.5 nm of the low-stiffness motors, force generation of single myosin molecules with hVLC^{E56G} may only be around 0.7 pN. There was no distinction in life time of all binding events. Besides the lever arm [24], the converter domain was suggested to represent an alternative element of elastic distortion during

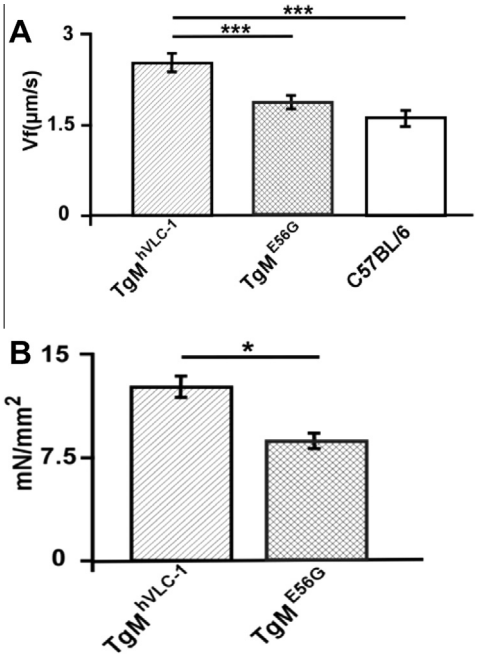

Fig. 3. In vitro motility assay and skinned fiber analysis. (A) Velocities of actin filaments (Vf) sliding of myosin purified from ventricles of 3 months old male C57BL/6 (3 animals, 123 actin filaments), TgM^{hVLC-1} (5 animals, 98 actin filaments) or TgM^{E56G} (4 animals, 60 actin filaments). (B) Isometric force generation expressed in mN/mm^2 cross-section of skinned fibers prepared from cardiac ventricles of 3 months old male TgM^{hVLC-1} (9 fibers) or TgM^{E56G} (10 fibers). Values are means ± SEM; $^{*}p < 0.05$, $^{***}p < 0.001$.

force generation [25]. A FHC-related mutation within the converter domain substantially decreased myosin stiffness in fibers [26,27]. 3D-analysis of myosin-S1 suggests close contacts between helix E of ELC with part of the converter domain [2,28], suggesting that ELC could modulate myosin stiffness also via converter domain interaction.

Similar to myosin stiffness and force, *in vitro* actin sliding velocity of ventricular myosin motors with different ELC forms decreased in the order hVLC-1 > hVLC-1^{E56G} ≈ mVLC-1. Myosin prepared from the ventricles of 3 months old male TgM^{hVLC-1} propelled actin filaments significantly ($p < 0.001$) faster [velocity of filament transportation (Vf) = 2.3 ± 0.13 µm/s; $n = 4$ animals, 123 filaments] than myosin prepared from TgM^{E56G} (Vf = 1.7 ± 0.07 µm/s; $n = 5$ animals, 98 filaments) (Fig. 3). Cardiac myosin prepared from C57BL/6 mice revealed an *in vitro* motility of 1.5 ± 0.03 µm/s ($n = 3$ animals, 89 filaments) which was significantly ($p < 0.001$) below the Vf observed with ventricular myosin prepared from TgM^{hVLC-1} mice (Fig. 3A). These reductions could not be due to an increased expression of β-MyHC, which propels actin filaments with a slower velocity than the α-MyHC [11,16]. We could not find any change of the ventricular MyHC isoenzyme expression, neither at the mRNA nor at the protein level.

Rather, *in vitro* actin sliding velocity (Vf) decreases if the duty time (ts) of XBs increases since Vf = *x*/ts [29]. Duty time is determined by the ADP release rate from the catalytic site, i.e. ts decreases if the ADP release rate increases [30]. In fact, similar to the shortening velocity of muscle fibers, Vf decreases with increasing ADP concentrations [31]. Modulation of the ADP release rate from the catalytic site of the myosin-MD by ELC is already suggested by experimental and structural data [32]. The 3D-structures of myosin-S-1 suggest close contacts between helix F and the N-terminal antenna of the ELC to the N-Terminus of the myosin-MD [2,28] [3]. Deletion of the N-terminal aa 1–80 of the myosin-MD destroyed normal ADP release rate of myosin II [33]. We, therefore suggest that the different ELC forms affects *in vitro* actin sliding velocity by modulation of the ADP release rate and/or a reduced value of x, i.e. the working stroke (c.f. above).

Loss-of-function of myosin and reduced *in vitro* velocity of actin sliding suggest deteriorated cardiac contractile parameters which are critically determined by interaction of myosin XBs with actin. Maximal isometric force obtained at maximal calcium activation level (pCa 4.5) of skinned fibers prepared from 3 months old male TgM^{E56G} was 8.3 ± 1.73 mN/mm^2 ($n = 10$ fibers), i.e. significantly ($p < 0.05$) lower than the force obtained from TgM^{hVLC-1} (13.9 ± 1.5 mN/mm^2; $n = 9$ fibers; Fig. 3B)). Calcium sensitivities expressed as pCa50 calculated from the tension/pCa curves of fibers prepared from TgM^{E56G} and TgM^{hVLC-1} was similar (5.44

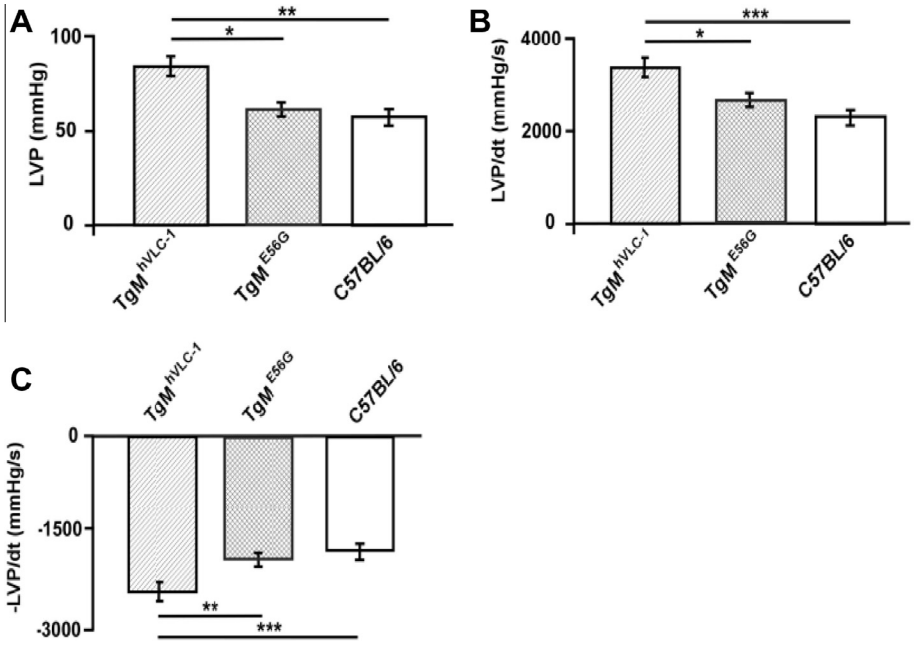

Fig. 4. Isolated perfused heart (Langendorff) measurements. (A) Maximal left ventricular isovolumetric pressure developments (LVP in mmHg) of TgM^{hVLC-1} ($n = 10$), TgM^{E56G} ($n = 9$) and C57BL/6 ($n = 9$). (B) Maximal rates of left ventricular isovolumetric pressure development (LVP/dt max. in mmHg/s). (C) Maximal relaxation rates of left ventricular isovolumetric pressure (−LVP/dt max. in mmHg/s). Values are expressed as means ± SEM, $^{*}p < 0.05$, $^{**}p < 0.01$, $^{***}p < 0.001$.

and 5.41, respectively). Accordingly, TgM^{E56G} and $TgM^{hVLC\text{-}1}$ fibers had similar Hill coefficient (3.5 and 3.2, respectively). The reduced force generation upon expression of hVLC-1^{E56G} is in agreement with a recent work showing that force of skinned heart fibers obtained from TgM^{A57G} decreased [34]. This predicts a "loss of function" of myosin with hVLC-1^{A57G} similar to the myosin with hVLC-1^{E56G} investigated herein and, therefore decreased stiffness. By contrast myosin stiffness of TgM^{A57G} rose [20], indicating a "gain of function" of myosin with hVLC-1^{A57G}. The reason for this discrepancy is yet unknown.

In addition, we investigated *in vitro* contractility of electrically paced isolated perfused hearts in the Langendorff-mode of TgM^{E56G}, $TgM^{hVLC\text{-}1}$ and C57BL/6. Isovolumetric pressure development of left ventricles (LVP) from hearts of TgM^{E56G} ($n = 10$) was 66.2 ± 4.2 mmHg. This was significantly lower compared to LVP of $TgM^{hVLC\text{-}1}$ (80.0 ± 4.6 mmHg; $n = 9$) (Fig. 4A). In addition, TgM^{E56G} revealed a significantly reduced maximal rate of isovolumetric pressure development (LVP_{dtmax} 2982.9 ± 194 mmHg/s) compared with $TgM^{hVLC\text{-}1}$ (LVP_{dtmax} 3613.2 ± 144 mmHg/s) (Fig. 4B) and significantly lower maximal rate of isovolumetric relaxation ($-LVP_{dtmax}$) compared with $TgM^{hVLC\text{-}1}$ ($-LVP_{dtmax}$ -− 1678.2 ± 140 mmHg/s vs. $-LVP_{dtmax}$ − 2465.1 ± 152 mmHg/s) (Fig. 4C). Interestingly, C57BL/6 mice ($n = 9$) revealed *in vitro* contractility parameters significantly lower than the levels observed in $TgM^{hVLC\text{-}1}$, i.e. LVP (59.3 ± 3.9 mmHg), LVP_{dtmax} (2453.4 ± 183 mmHg/s) and $-LVP_{dtmax}$ (−1553.2 ± 138 mmHg/s) (Fig. 4A–C). Coronary flow of isolated perfused hearts was similar among all three groups (2.1 ± 0.1, 1.9 ± 0.3, and 2.2 ± 0.4 ml/min in $TgM^{hVLC\text{-}1}$, TgM^{E56G} and C57BL/6, respectively.

The deleterious effects of the E56G mutated hVLC-1 on myosin and cardiac functions described herein may represent a valuable molecular pathomechanism provoking the development of FHC upon hVLC-1 mutations. Those mutations may weaken the myosin-LA affinity, reduce stiffness and unitary force generation of the single myosin molecule, slow down actin filament sliding velocity, and depress cardiac performance. The resulting cardiac hypocontractility could then activate hypertrophic pathways leading to the FHC phenotype [35].

Taken together, we provide a molecular mechanism which could explain the physiological regulation of myosin force generation by various ELC forms, namely via distinct myosin-LA affinity which may determine myosin stiffness and, therefore myosin and cardiac functions.

Acknowledgments

We gratefully acknowledge Petra Sakel, Petra Domaing and Steffen Lutter for technical assistance. This work was supported by DFG GK 754 to J.L. and I.M; DFG STE 1697/2 to W.S. and the German Center for Cardiovascular Research (DZHK) to VRZ.

Appendix A. Supplementary data

Supplementary data associated with this article can be found, in the online version, at http://dx.doi.org/10.1016/j.bbrc.2014.05.142.

References

[1] E.M. Aydt, G. Wolff, I. Morano, Molecular modeling of the myosin-S1(A1) isoform, J. Struct. Biol. 159 (2007) 158–163.
[2] I. Rayment, H.M. Holden, M. Whittaker, et al., Structure of the actin–myosin complex and its implications for muscle contraction, Science 261 (1993) 58–65.
[3] S. Lowey, L.D. Saraswat, H. Liu, et al., Evidence for an interaction between the SH3 domain and the N-terminal extension of the essential light chain in class II myosins, J. Mol. Biol. 371 (2007) 902–913.
[4] R. Bottinelli, R. Betto, S. Schiaffino, et al., Unloaded shortening velocity and myosin heavy chain and alkali light chain isoform composition in rat skeletal muscle fibres, J. Physiol. 478 (Pt 2) (1994) 341–349.
[5] P. VanBuren, G.S. Waller, D.E. Harris, et al., The essential light chain is required for full force production by skeletal muscle myosin, Proc. Natl. Acad. Sci. U.S.A. 91 (1994) 12403–12407.
[6] S. Lowey, G.S. Waller, K.M. Trybus, Skeletal muscle myosin light chains are essential for physiological speeds of shortening, Nature 365 (1993) 454–456.
[7] O.M. Hernandez, M. Jones, G. Guzman, et al., Myosin essential light chain in health and disease, Am. J. Physiol. Heart Circ. Physiol. 292 (2007) H1643–H1654.
[8] G. Piazzesi, M. Reconditi, M. Linari, et al., Skeletal muscle performance determined by modulation of number of myosin motors rather than motor force or stroke size, Cell 131 (2007) 784–795.
[9] J. Howard, J.A. Spudich, Is the lever arm of myosin a molecular elastic element?, Proc Natl. Acad. Sci. U.S.A. 93 (1996) 4462–4464.
[10] R.J. Solaro, D.C. Pang, F.N. Briggs, The purification of cardiac myofibrils with Triton X-100, Biochim. Biophys. Acta 245 (1971) 259–262.
[11] M. Canepari, R. Rossi, M.A. Pellegrino, et al., Speeds of actin translocation in vitro by myosins extracted from single rat muscle fibres of different types, Exp. Physiol. 84 (1999) 803–806.
[12] U. Carraro, C. Catani, A sensitive SDS–PAGE method separating myosin heavy chain isoforms of rat skeletal muscles reveals the heterogeneous nature of the embryonic myosin, Biochem. Biophys. Res. Commun. 116 (1983) 793–802.
[13] A. Lewalle, W. Steffen, O. Stevenson, et al., Single-molecule measurement of the stiffness of the rigor myosin head, Biophys. J. 94 (2008) 2160–2169.
[14] D.A. Smith, W. Steffen, R.M. Simmons, et al., Hidden-Markov methods for the analysis of single-molecule actomyosin displacement data: the variance-Hidden-Markov method, Biophys. J. 81 (2001) 2795–2816.
[15] W. Steffen, D. Smith, R. Simmons, et al., Mapping the actin filament with myosin, Proc. Natl. Acad. Sci. U.S.A. 98 (2001) 14949–14954.
[16] M. Canepari, R. Rossi, M.A. Pellegrino, et al., Functional diversity between orthologous myosins with minimal sequence diversity, J. Muscle Res. Cell Motil. 21 (2000) 375–382.
[17] I. Morano, F. Hofmann, M. Zimmer, et al., The influence of P-light chain phosphorylation by myosin light chain kinase on the calcium sensitivity of chemically skinned heart fibres, FEBS Lett. 189 (1985) 221–224.
[18] J. James, Y. Zhang, K. Wright, et al., Transgenic rabbits expressing mutant essential light chain do not develop hypertrophic cardiomyopathy, J. Mol. Cell Cardiol. 34 (2002) 873–882.
[19] A. Sanbe, D. Nelson, J. Gulick, et al., In vivo analysis of an essential myosin light chain mutation linked to familial hypertrophic cardiomyopathy, Circ. Res. 87 (2000) 296–302.
[20] P. Muthu, L. Wang, C.C. Yuan, et al., Structural and functional aspects of the myosin essential light chain in cardiac muscle contraction, FASEB J. 25 (2011) 4394–4405.
[21] M. Linari, M. Caremani, C. Piperio, et al., Stiffness and fraction of myosin motors responsible for active force in permeabilized muscle fibers from rabbit psoas, Biophys. J. 92 (2007) 2476–2490.
[22] M. Capitanio, M. Canepari, P. Cacciafesta, et al., Two independent mechanical events in the interaction cycle of skeletal muscle myosin with actin, Proc. Natl. Acad. Sci. U.S.A. 103 (2006) 87–92.
[23] C. Veigel, M.L. Bartoo, D.C. White, et al., The stiffness of rabbit skeletal actomyosin cross-bridges determined with an optical tweezers transducer, Biophys. J. 75 (1998) 1424–1438.
[24] T.Q. Uyeda, P.D. Abramson, J.A. Spudich, The neck region of the myosin motor domain acts as a lever arm to generate movement, Proc. Natl. Acad. Sci. U.S.A. 93 (1996) 4459–4464.
[25] I. Dobbie, M. Linari, G. Piazzesi, et al., Elastic bending and active tilting of myosin heads during muscle contraction, Nature 396 (1998) 383–387.
[26] J. Kohler, G. Winkler, I. Schulte, et al., Mutation of the myosin converter domain alters cross-bridge elasticity, Proc. Natl. Acad. Sci. U.S.A. 99 (2002) 3557–3562.
[27] B. Seebohm, F. Matinmehr, J. Kohler, et al., Cardiomyopathy mutations reveal variable region of myosin converter as major element of cross-bridge compliance, Biophys. J. 97 (2009) 806–824.
[28] R.A. Milligan, Protein–protein interactions in the rigor actomyosin complex, Proc. Natl. Acad. Sci. U.S.A. 93 (1996) 21–26.
[29] T.Q. Uyeda, S.J. Kron, J.A. Spudich, Myosin step size. Estimation from slow sliding movement of actin over low densities of heavy meromyosin, J. Mol. Biol. 214 (1990) 699–710.
[30] R.F. Siemankowski, M.O. Wiseman, H.D. White, ADP dissociation from actomyosin subfragment 1 is sufficiently slow to limit the unloaded shortening velocity in vertebrate muscle, Proc. Natl. Acad. Sci. U.S.A. 82 (1985) 658–662.
[31] E. Homsher, F. Wang, J.R. Sellers, Factors affecting movement of F-actin filaments propelled by skeletal muscle heavy meromyosin, Am. J. Physiol. 262 (1992) C714–C723.
[32] J. Borejdo, D.S. Ushakov, R. Moreland, et al., The power stroke causes changes in the orientation and mobility of the termini of essential light chain 1 of myosin, Biochemistry 40 (2001) 3796–3803.
[33] S. Fujita-Becker, G. Tsiavaliaris, R. Ohkura, et al., Functional characterization of the N-terminal region of myosin-2, J. Biol. Chem. 281 (2006) 36102–36109.
[34] K. Kazmierczak, E.C. Paulino, W. Huang, et al., Discrete effects of A57G-myosin essential light chain mutation associated with familial hypertrophic cardiomyopathy, Am. J. Physiol. Heart Circ. Physiol. 305 (2013) H575–H589.
[35] H. Ashrafian, C. Redwood, E. Blair, et al., Hypertrophic cardiomyopathy: a paradigm for myocardial energy depletion, Trends Genet. 19 (2003) 263–268.